Chikungunya virus non-structural protein 2 (nsP2) inhibits RIG-I and TLR-mediated immune response

Shivani Raj[1], Minnah Irfan[1], C.T. Ranjith-Kumar[1*]
[1]University School of Biotechnology, Guru Gobind Singh Indraprastha University, Sec-16C, Dwarka, New Delhi, India 110078
*Corresponding author email: ctrkumar@ipu.ac.in

Abstract

Chikungunya virus (CHIKV) is a single-stranded positive-sense RNA virus that employs various strategies to evade the host's immune response. The CHIKV non-structural protein 2 (nsP2) is one of the viral-encoded proteins essential for viral replication as well as modulation of the immune response. In this study, we demonstrate that CHIKV nsP2 suppresses both RIG-I-like receptors (RLR) and Toll-like receptors (TLR) signaling pathways. Domain mapping of the nsP2 identified the N-terminal region encompassing the N-terminal domain and the helicase domain (NH) is responsible for the inhibition. Furthermore, site-directed mutagenesis experiments showed that functional helicase is necessary for inhibiting interferon production, but the C-terminal V-Loop region, previously implicated in host transcriptional shutoff, is not. In addition, nsP2 disrupts two key immune signaling pathways: RLR and TLRs, by blocking common proteins such as TBK1 and IRF3.

Importance

Our research provides critical insights into the mechanisms by which CHIKV evades host immune response, specifically through the actions of its non-structural protein 2 (nsP2). While viral proteins are known to suppress innate immune responses to facilitate replication, the precise role of how CHIKV nsP2 interferes remains unclear. Here, we demonstrate that nsP2 disrupts two key immune signaling pathways, RLR and TLRs, by interfering with common proteins such as TBK1 and IRF3 involved in both signaling pathways. These findings enhance our understanding of CHIKV immune evasion strategies and offer potential targets for the development of antiviral therapeutics.

Keywords – nsP2, RIG-I signaling, helicase, V-Loop

Introduction

CHIKV belongs to the *Alphavirus* genus within *Togaviridae* family and causes acute febrile illness known as chikungunya fever in humans. It is an arthropod-borne virus primarily transmitted by *Aedes albopictus* and *Aedes aegypti* mosquitoes (1). CHIKV has a positive-sense single-stranded RNA genome of 11.8kb. The CHIKV genome contains two open reading frames (ORFs). ORF1 is processed into four non-structural proteins (nsP1, nsP2, nsP3, and nsP4) essential for virus replication and RNA transcription. While ORF2 is processed into structural proteins (C, E1, E2, E3, and 6K protein) (2).

The innate immune response is the first line of defense against viral infection. Activation of the immune response leads to the production of interferons and cytokines, which limit the replication of the virus (3). Viral proteins not only play a crucial role in replication but also use multiple strategies to disrupt cellular mechanisms, allowing viruses to evade immune response and establish infection. Detection of viral RNA or pathogen-associated molecular patterns (PAMPs) is mediated by Pathogen recognition receptors (PRRs), like TLRs and RLRs (4-7). These PRRs recognize viral RNA and replication intermediates and trigger downstream signaling through adaptor proteins like mitochondrial antiviral signaling

(MAVS) for RLR receptor, while TLRs use TIR-domain-containing adaptor inducing interferon β (TRIF) and myeloid differentiation primary response gene 88 (MyD88) (7, 8). This triggers a cascade of signaling that activates TANK-binding kinase 1 (TBK1), which further phosphorylates the interferon regulatory factor 3 (IRF3), ultimately leading to the production of interferons and cytokines (9).

Like many alphaviruses, CHIKV uses both non-structural and structural proteins to evade the immune response (10). nsP2 is a multifunctional protein necessary for viral replication and is known to interfere with the immune response (11). The N-terminus of CHIKV nsP2 possesses nucleoside triphosphatase, helicase, and RNA-dependent 5-triphosphatase activity, while the C-terminus harbors a protease domain and methyltransferase-like domain (MTase) (12, 13). Structurally, the N-terminal region is further classified into the N-terminal domain (NTD), Stalk α-helix, and accessory domains 1B, all of which wrap around the conserved helicase core, ensuring conformational stability (14). Notably, the first 14 amino acids of the N-terminal region play a crucial role in stabilizing the structure and helicase activity; disruption in this region results in impairment of the function (14, 15).

The helicase domain is involved in unwinding of viral RNA during replication and transcription (16). Mutations within conserved helicase motifs significantly impair its functioning (17-19). CHIKV nsP2 helicase is a member of the helicase superfamily 1 (SF1) and contains seven conserved signature motifs (I, Ia, II, III, IV, V, and VI), which form the enzyme's catalytic core (20). The Walker A motif is characterized by lysine residues and binds the β- and γ-phosphates of NTP-Mg^{2+}, while the Walker B motif contains a conserved aspartate residue that interacts with Mg^{2+} (12, 15). In addition, the C-terminal region of the nsP2 harbors a segment called V-Loop (residues A674, T675, and L676), which has been shown to degrade RNA polymerase II subunit Rpb1, leading to host transcription shutoff (21).

Thus, CHIKV employs various strategies to evade immune response, with nsP2 playing a crucial role in suppressing innate immunity. However, the precise molecular mechanism underlying this immune evasion is not well understood. In this study, we sought to elucidate the role of nsP2's functional domains in immune inhibition by generating various deletion mutants. Furthermore, we introduced targeted mutations in the conserved Walker motifs to disrupt helicase activity, as well as in the C-terminal V-Loop region, previously implicated in host transcriptional shutoff. Our findings indicate that the N-terminal domain and helicase domain (NH) of the protein is crucial for nsP2-mediated immune suppression and is not dependent on host transcriptional shutoff, highlighting a novel functional aspect of this viral protein. By uncovering the mechanisms through which nsP2 impairs interferon and pro-inflammatory cytokine production, this study enhances our understanding of CHIKV pathogenesis and provides a foundation for the development of targeted antiviral strategies.

Results

nsP2 inhibits the RIG-I signaling

To assess whether any of the CHIKV non-structural protein(s) interferes with the RIG-I signaling, each of the nsPs (nsP1, nsP2, nsP3, and nsP4) were cloned into the mammalian expression vector pUNO-MCS, and their expression was confirmed by Western blotting using anti-FLAG antibody [Fig. 1A]. Effect of CHIKV nsP(s) on RIG-I signaling was determined by dual luciferase reporter assay as described earlier (22). Briefly, HEK293T cells were co-transfected with each of the nsPs along with the plasmid expressing full-length RIG-I receptor and luciferase reporter plasmids. 24h post-transfection, 5' triphosphorylated

dsRNA of 27bp (3PdsRNA) was used to activate RIG-I signaling (23). The reporter plasmids expressing firefly luciferase under the IFN-β promoter (IFNβ-luc) was used to measure IFN-β promoter activation and *Renilla* luciferase under the thymidine kinase promoter (phRLTKLuc) used as an internal control (24). Results show that nsP2 inhibited RIG-I signaling significantly while other nsPs showed minimal or no effect [Fig. 1B]. To analyze whether nsP2 specifically targets RIG-I receptor or its downstream signaling, we transfected the constitutively active mutant of RIG-I, consisting of only its CARD domains (R-C) instead of full-length RIG-I [Fig. 1C]. R-C was co-transfected along with individual non-structural proteins, and similar to the inhibition of 3PdsRNA-induced RIG-I signaling, nsP2 inhibited R-C-induced signaling, suggesting that nsP2 could be blocking the CARD domains of RIG-I or at a step further downstream [Fig. 1C]. Further, a WST-I (Water Soluble Tetrazolium 1) assay was carried out to confirm that the observed inhibition was not due to cytotoxicity [Fig. 1D]. No cytotoxic effect was observed, further confirming that nsP2's inhibitory effect on RIG-I signaling was not due to any cell damage. Additionally, qRT-PCR analysis was performed to determine the effect of nsP2 at the transcriptional levels of IFN-β, which as expected, revealed a significant reduction in the IFN-β mRNA, confirming the nsP2-mediated inhibition of RIG-I signaling [Fig. 1E]. These data suggest that nsP2 is involved in inhibiting the RIG-I signaling pathway.

NH region of CHIKV nsP2 is involved in the inhibition of RIG-I signaling.

In order to identify the specific region of nsP2 responsible for RIG-I inhibition, following deletion mutants of nsP2- NTD (1-167 aa), H (167-470 aa), NH (1-470 aa), HP (167-605 aa), NHP(1-605 aa), HPM(167-798 aa), P(470-605 aa), PM(470- 798aa), and M(605-798 aa) were constructed in the mammalian expression vector pUNO-MCS [Fig. 2A]. Protein expression was confirmed by western blotting using an anti-flag antibody [Fig. 2B]. For analyzing the effect of subdomains of nsP2 on RIG-I signaling, IFNβ promoter activity was measured through dual luciferase reporter assay [Fig. 2C]. The N-terminal domain and the helicase domain (NH) region showed similar inhibition of RIG-I signaling as that of a full-length nsP2, while the other domains showed significantly less inhibition. This suggests that NH might be the primary region of nsP2 necessary for inhibition. A quantitative RT-PCR was performed to measure IFNβ mRNA levels to verify the observed inhibition by nsP2 and NH. As expected, the NH domain showed similar inhibition as full-length nsP2, further confirming that the NH domain within nsP2 is sufficient for inhibiting RIG-I signaling [Fig. 2D]. Lastly, to assess the potency of observed inhibition, HEK293T cells were co-transfected with increasing amounts of nsP2 and NH (10ng to 250ng) plasmids along with R-C [Fig. 2E and 2F]. As evident from Fig. 2E and 2F, at lower amounts of plasmids, nsP2 was more potent in inhibiting RIG-I signaling compared to NH. Taken together, our data suggest that while NH is an important region for inhibiting RIG-I signaling, the other domains may also be needed by the nsP2 for efficient inhibition.

Minimal region of NH involved in the inhibition of RIG-I signaling.

The N-terminal region is classified into subregions NTD (77aa), stalk (77aa-110aa), and 1B (110aa-175aa), which are the accessory domains of nsP2 necessary for helicase activity (14). To identify the minimal region of nsP2 necessary for the observed inhibition, further mutants of NH were generated wherein N-terminal 14aa (Δ14 NH), 77aa (Δ77 NH), and 110aa (Δ110 NH) were deleted [Fig. 3A]. The deletion mutants were cloned in pUNO-MCS mammalian expression vector, and their expression was confirmed using western analysis [Fig. 3B]. The impact of these deletion mutants on RIG-I signaling was assessed by dual luciferase reporter assay and was further validated by qRT-PCR [Fig. 3C & 3D]. Interestingly, the N-terminal

deletion mutants showed no significant inhibition compared to NH in both dual luciferase and qRT-PCR assays [Fig. 3C & D]. These data indicate that the entire N-terminal domain and Helicase domain(NH) might be important for the observed inhibition of RIG-I signaling.

nsP2 requires helicase activity to inhibit RIG-I signaling

Since the N-terminal region of nsP2 is shown to be crucial for the stability and helicase activity of nsP2 (14), we investigated whether helicase activity contributes to nsP2's inhibition of RIG-I signaling. Firstly, we performed comparative sequence analysis of the helicase region among various alphaviruses, which as expected, revealed that Walker A and B motifs are highly conserved [Fig. 4A]. We further compared the helicase domain of some other RNA viruses and found the Walker A motif is conserved among them as well [Fig. 4B]. These conserved domains were subjected to mutational analysis, wherein Walker A (K192A) and Walker B (D252A, DE252/253AA) motif mutants critical for the helicase function were generated, and their expression was confirmed by western analysis [Fig. 4C]. To assess the role of Walker motif mutants on RIG-I signaling, a dual luciferase reporter assay was performed to measure IFN-β promoter activity [Fig. 4D]. Compared to the wild-type (WT) nsP2,-Walker motif mutants showed no inhibition of the RIG-I signaling, suggesting that the helicase activity of nsP2 is important for inhibition. This was further confirmed by analyzing IFNβ mRNA levels through qRT-PCR [Fig. 4E].

V-Loop region of the C-terminal domain of nsP2 is not necessary for the inhibition of innate immune response

Next, we focused on the C-terminal portion of nsP2. The C-terminal domain of nsP2, specifically the V-loop region (674 to 676 aa), has previously been reported to be involved in the host transcriptional shutoff by the degrading catalytic subunit of RNAPII, Rpb1 (25, 26). To investigate whether host-transcriptional shutoff contributes to the inhibition of RIG-I signaling, we focused on the V-Loop region. First, comparative sequence analysis of the V-Loop region among various alphaviruses was performed using Clustal Omega (27), which revealed sequence conservation among alphaviruses [Fig. 5A]. Akhrymuk et al., 2019 have shown that substitution mutation of the amino acids A, T, and L in the VLoop of CHIKV nsP2 into R, L, and E amino acids negatively impacted the host transcriptional shutoff by the virus (28). To assess potential structural change caused by this mutation, we predicted and compared the structure of WT-nsP2 and nsP2 RLE mutant using AlphaFold (29). The RLE mutation disrupted the structure of V-Loop region of nsP2 as shown in Fig. 5B. For understanding the role of host transcriptional shutoff and to validate whether a change in structure has any impact on the inhibition of IFNβ signaling, the V-Loop RLE mutant was generated in pUNO-MCS and protein expression was confirmed by Western analysis [Fig. 5C]. To determine its effect on RIG-I signaling, IFNβ promoter activation and mRNA levels were measured by dual luciferase reporter assay and qRT-PCR, respectively [Fig. 5D & 5E]. Similar inhibition of RIG-I signaling was observed by nsP2 RLE mutant as wild-type nsP2. This suggests that the host transcriptional shutoff by nsP2's V-Loop region may not be involved in the inhibition of RIG-I signaling.

nsP2 and NH inhibit IPS-I, TRIF, and MyD88-induced IFNβ production

Next, we investigated whether nsP2 and NH target the RIG-I receptor directly to inhibit signaling. For this, we first assessed nsP2's impact on the adaptor protein of RIG-I signaling, IPS-I (also known as MAVS, Cardiff, VISA) (30). Overexpression of IPS-I mimics the activation of RIG-I signaling (31, 32). Upon co-expression, both nsP2 and NH inhibited IPS-1-induced signaling significantly in both dual luciferase assay and qRT-PCR [Fig. 6A and

6D] suggesting that nsP2 and NH does not directly interact with RIG-I protein but might be interfering with signaling events downstream of the RIG-I receptor.

To further elucidate whether the observed inhibition is specific to RIG-I signaling, we examined the impact of nsP2 and NH on the adaptor proteins of TLRs, namely TRIF and MyD88. TRIF is the adaptor for TLR3, and MyD88 is the adaptor for all other TLRs. However, TLR4 uses both TRIF and MyD88 for signalling. Similar to IPS-1, overexpression of these adaptor proteins will mimic TLR signaling (32). nsP2, and NH showed inhibition of the signaling induced by both TRIF and MyD88 in both dual luciferase reporter assay and qRT-PCR [Fig. 6B,6C and 6E, 6F]. This indicates that nsP2 and NH interfere with the signaling components common to both the TLR and RLR signaling pathways, perhaps targeting common proteins involved in these pathways.

Effect of nsP2 and NH on IRF3 and TBK1

Having shown that nsP2 inhibits both RLR and TLR pathways, we next looked at the possible common proteins involved in these pathways. For this, we investigated the effect of nsP2 on TBK1 and IRF3, which are known to be involved in both RLR and TLR signaling pathways (9). To analyze whether nsP2 and NH target these proteins, IFNβ promoter activation was measured through dual luciferase reporter assay by overexpressing TBK1 and IRF3 in the presence and absence of nsP2 and NH [Fig. 7A,7B]. nsP2 and NH showed significant suppression of TBK1 and IRF3-induced signaling, which was further confirmed by analyzing IFNβ mRNA levels by qRT-PCR [Fig. 7C and 7D]. This suggests that nsP2 and NH might be targeting common proteins involved in both RLR and TLR signaling pathways.

Taken together, our data suggest that the N-terminal domain and the helicase domain(NH) of the nsP2 is sufficient to inhibit both RLR and TLR signaling, and this inhibition requires a functional helicase domain. Furthermore, our findings suggest that nsP2-mediated inhibition occurs independently of host transcriptional shutoff.

Discussion

The production of IFNs and cytokines is a crucial component of the innate immune response against viral infection (33). The PRRs detect PAMPs, such as viral replication intermediates, triggering the production of type I and type III IFNs, along with various cytokines and chemokines (4). Among the diverse PRRs, RLRs and TLRs play critical roles in recognizing the viral replication intermediates, including dsRNA, ssRNA, and short 5’ triphosphate RNAs (3, 34). RNA viruses have evolved various strategies to evade immune detection and modulate signaling pathways, often employing both structural and non-structural proteins to disrupt host immune response and ensure viral survival (35). Understanding these viral mechanisms is crucial for developing antiviral strategies against viral infection.

Previous studies have established that nsP2 of alphaviruses, including CHIKV, not only plays a role in viral replication but also modulates host cellular pathways by interfering with components of immune signaling to evade the host immune response (25, 26, 36). Our findings demonstrate that CHIKV nsP2 inhibits immune response by suppressing signaling by key adaptor proteins, such as IPS-I for RLR and MyD88 and TRIF for TLRs, suggesting that nsP2 targets common signaling intermediates in these pathways. We hypothesized that nsP2 may interfere with common downstream proteins such as TBK1 and IRF3, which are essential for the production of interferons and cytokines. Overexpression studies with these proteins revealed that nsP2 suppresses TBK1 and IRF3-mediated signaling, which implies that nsP2 targets common proteins, either through direct interaction or by modulating other components to suppress RLR and TLR-mediated immune response.

Domain mapping of nsP2 further revealed that the N-terminal domain and the helicase domain (NH) of nsP2 are sufficient to mediate the inhibition of RLR and TLR signaling, although inhibition by the full-length nsP2 is more substantial [Fig. 2C]. However, NH alone showed much lower inhibition compared to full-length nsP2 at lower amounts of plasmid [Fig. 2E and 2F]. This indicates that full-length nsP2 may exhibit higher affinity or interaction with host target protein(s) involved in these pathways, thereby contributing more effectively to the inhibition of the immune response. This is further substantiated by the observation that domains other than the NH of nsP2 also showed inhibition, though to a much lesser extent [Fig. 2C]. Interestingly, the first 14 amino acids of the N-terminal region of nsP2 were found to be crucial for suppressing RIG-I signaling. Previously, this region was reported to be important for NTPase and helicase activities and to stabilize the structure of nsP2 (14). These findings also reveal the importance of helicase activity in the inhibition of RLR and TLR signaling.

Viral helicases are crucial for the unwinding of RNA during replication, but they have also been shown to interfere with the innate immune response (37, 38). In several viruses, helicase domains contribute to immune evasion, like the NS3 helicase of the Hepatitis C virus (HCV), which directly interacts with TBK1, preventing activation of IRF3 and leading to suppression of interferon production (39). Similarly, Riedl et al., 2019 demonstrated that the helicase domains of NS3 from Zika Virus (ZIKV), Dengue Virus (DENV), and West Nile Virus (WNV) disrupt the interaction between scaffold protein 14-3-3 and RIG-I during antiviral response, resulting in attenuated host immune response (40, 41). Likewise, the nsp13 helicase of SARS-CoV-2 blocks the interaction of TBK1 and IRF3 to disrupt the signaling (42, 43). Mutational analysis of SARS-CoV-2 nsp13 helicase revealed that a functional helicase is critical for nucleic acid binding. Disruption of this impairs STAT1 phosphorylation, thereby suppressing the immune response (43). In addition, NS3 helicase of WNV interferes with the innate immune response by inhibiting STAT1 phosphorylation (44). These findings highlight the role of helicase in immune evasion across viruses. Similarly, our mutational analysis in conserved helicase walker motifs (Walker A and Walker B) of the CHIKV, necessary for ATP hydrolysis and viral RNA replication, prevented nsP2 from inhibiting RIG-I signaling. This further highlights that helicase activity is essential for the CHIKV nsP2-mediated interference with the immune signaling.

CHIKV nsP2 C-terminal has previously been associated with antagonizing the JAK-STAT signaling pathway and also in promoting the degradation of RNA polymerase II subunit, RbP1, leading to the shutoff of host transcription (21, 45, 46) . However, our data demonstrated that the NH region alone is sufficient to inhibit the RIG-I and TLR signaling, suggesting that the transcriptional shutoff may not be necessary for inhibition of interferon response. Meshram et al., 2019 (26) reported that substitution mutations in the V-Loop, wherein amino acids A, T, and L were substituted with R, L, and E, failed to induce transcriptional shutoff and also did not affect viral replication (28). The structure prediction and comparison of WT-nsP2 and nsP2 RLE mutant revealed disruption of the loop structure in the mutant. This structural perturbation could contribute to the lack of mutant's ability to shut off host transcription. Further, this RLE mutation in CHIKV nsP2 inhibited RIG-I signaling similar to wild type [Fig. 5], indicating that host transcriptional shutoff is not a contributing factor for the interference of innate immune response. This further validates the role of the NH encompassing the active helicase domain of nsP2, which interferes with RLR and TLR signaling.

In conclusion, our study shows that CHIKV nsP2 is a major antagonist of the interferon production induced by RLR and TLR signaling pathways. nsP2 likely targets common points downstream of the TLR and RLR signaling to suppress interferon production, although further studies are required to identify the target protein. The requirement for functional helicase and the pivotal role of the NH region in this inhibition provide new insights into the molecular mechanisms. These insights into CHIKV's evasion of host defense could potentially provide targets for developing antiviral strategies and therapeutics against CHIKV infection.

Material and methods

Plasmid construct:

Plasmids encoding C-terminal FLAG-tagged CHIKV non-structural proteins (nsP1, nsP2, nsP3, nsP4), subdomains of nsP2 (NTD, NH, H, HPM, NHP, HP, P, M), and deletion constructs of NH (Δ14 NH, Δ77 NH, Δ110 NH were generated by subcloning into pUNO (Invivogen) expression vector. Helicase mutants (K192A, D252A, and DE252/253AA) were generated using site-directed mutagenesis and cloned into pUNO-MCS. Similarly, RLE mutant (V-Loop) was also generated. Clones were generated by PCR using CHIKV strain IND-06-Guj as a template. Both the vector pUNO and the PCR products were digested using *AgeI* and *NheI* restriction enzymes. The digested PCR products and vector were ligated, and the ligated products were transformed and expressed in *E.coli* Top10 cells. Further clones were subjected to full-length DNA sequencing. Primer sequences will be available upon request.

Maintenance of Cell lines

HEK293T cells and Huh7 cells were maintained in Dulbecco's Modified Eagle Medium (DMEM) supplemented with 10 % Fetal Bovine Serum (FBS) and penicillin/streptomycin at 37 $^{\circ}$C, 5% CO_2. For transfection, cells were seeded at 70-80% confluency.

Dual-Luciferase Assay

The day prior to transfection, HEK293T cells (20,000 cells/well) were seeded into a CoStar White 96-well plate. Cells were co-transfected with Firefly luciferase cloned under the IFN-β promoter (IFNβ-luc) was used as the reporter to measure the IFN-β promoter induction. Renilla luciferase cloned under thymidine kinase promoter (phRLTKLuc) was used as an internal control. To induce RIG-I signaling, RIG-I was co-transfected with the plasmids of nsPs, which was activated using 3pdsRNA post 24hr of transfection. For further experiments, CARD domain mutant (R-C) was used instead of RIG-I as its overexpression mimics RIG-I signaling. According to the manufacturer's protocol, HEK293T cells were transfected with varying amounts of plasmids using Lipofectamine 2000. DualGlo Luciferase assay system reagents were used to detect the luciferase activity 48 hours after transfection.

Cytotoxic Assay

40,000 HEK293T cells were seeded per well into a CoStar White 96-well plate and grown overnight at 37 °C. After 16 hrs, cells were transfected with different amounts of nsP2 plasmid using Lipofectamine 2000 according to the manufacturer's protocol. After 24 hrs, the media was removed, and WST-reagent was used to measure the viability of cells. Absorbance was measured at 450nm and 630 nm using an ELISA absorbance reader.

RT-PCR

To analyze the expression of downstream IFNβ induced by R-C signaling by Real-time PCR. HEK293T cells were seeded in 12 12-well plate with 400,000 cells per well, one day before the transfection. The next day, cells were transfected with the R-C in the presence and absence of nsP2 using Lipofectamine 2000 according to the manufacturer's protocol. 48h post-transfection, total RNA was isolated using RNAiso Plus reagent (TAKARA) according to the manufacturer's protocol. cDNA synthesis was performed for the total RNA isolated using random hexamers according to the manufacturer's protocol (PrimeScript 1st strand cDNA synthesis kit, Takara bio companies). Quantitative Real-Time PCR (qRT-PCR) was carried out using gene-specific primers to quantify mRNA levels of IFNβ. Ct values corresponding to IFNβ mRNA levels measured and normalized with GAPDH Ct values and change in mRNA levels was calculated by ΔΔCt method with respect to vector control.

Western Blotting

HEK293T cells were transfected with the plasmids of clones generated. Post 48h transfection, transfected cells were washed with the 1ml PBS, lysed with Laemmli buffer, and kept at 95°C for 10 mins. Lysate of transfected cells were loaded into well of 12% polyacrylamide gel. SDS-PAGE separated the proteins and then transferred them to a nitrocellulose membrane and detected them using an anti-FLAG antibody (1:2000). Detection of the antibody-protein complex was done using an ECL western blotting kit according to the manufacturer's protocol.

Statistical analysis

All data were analyzed using GraphPad Prism software. Statistical analysis between groups was conducted using a t-test. The differences among samples were considered significant for the values <0.05.

Acknowledgments

This work was funded by the Faculty Research Grant Scheme (FRGS) of Guru Gobind Singh Indraprastha (2022-2025) and was partly funded by the Council of Scientific and Industrial Research (CSIR). Indian Council of Medical Research (ICMR) funded the fellowship of Shivani Raj (Senior Research Fellowship). We thank Professor Sudhanshu Vrati, Regional Center for Biotechnology (RCB) and Dr. Milan Surjit from Translational Health Science and Technology Institute (THSTI) for their valuable help. The authors declare no conflict of interest.

References

1. Vairo F, Haider N, Kock R, Ntoumi F, Ippolito G, Zumla A. 2019. Chikungunya: epidemiology, pathogenesis, clinical features, management, and prevention. Infectious Disease Clinics 33:1003-1025.
2. Silva LA, Dermody TS. 2017. Chikungunya virus: epidemiology, replication, disease mechanisms, and prospective intervention strategies. The Journal of clinical investigation 127:737-749.
3. Rai KR, Shrestha P, Yang B, Chen Y, Liu S, Maarouf M, Chen J-L. 2021. Acute infection of viral pathogens and their innate immune escape. Frontiers in microbiology 12:672026.
4. Carty M, Guy C, Bowie AG. 2021. Detection of viral infections by innate immunity. Biochemical pharmacology 183:114316.

5. Okamoto M, Tsukamoto H, Kouwaki T, Seya T, Oshiumi H. 2017. Recognition of viral RNA by pattern recognition receptors in the induction of innate immunity and excessive inflammation during respiratory viral infections. Viral immunology 30:408-420.
6. Yoneyama M, Onomoto K, Jogi M, Akaboshi T, Fujita T. 2015. Viral RNA detection by RIG-I-like receptors. Current opinion in immunology 32:48-53.
7. Wicherska-Pawłowska K, Wróbel T, Rybka J. 2021. Toll-like receptors (TLRs), NOD-like receptors (NLRs), and RIG-I-like receptors (RLRs) in innate immunity. TLRs, NLRs, and RLRs ligands as immunotherapeutic agents for hematopoietic diseases. International journal of molecular sciences 22:13397.
8. Kawai T, Akira S. 2008. Toll-like receptor and RIG-1-like receptor signaling. Annals of the New York Academy of Sciences 1143:1-20.
9. Fitzgerald KA, McWhirter SM, Faia KL, Rowe DC, Latz E, Golenbock DT, Coyle AJ, Liao S-M, Maniatis T. 2003. IKKε and TBK1 are essential components of the IRF3 signaling pathway. Nature immunology 4:491-496.
10. Liu Y, Yuan Y, Zhang L. 2022. Innate immune evasion by alphaviruses. Frontiers in Immunology 13:1005586.
11. Wang S, Mahalingam S, Merits A. 2025. Alphavirus nsP2: A Multifunctional Regulator of Viral Replication and Promising Target for Anti-Alphavirus Therapies. Reviews in Medical Virology 35:e70030.
12. Karpe YA, Aher PP, Lole KS. 2011. NTPase and 5′-RNA triphosphatase activities of Chikungunya virus nsP2 protein. PloS one 6:e22336.
13. Fros JJ, van der Maten E, Vlak JM, Pijlman GP. 2013. The C-terminal domain of chikungunya virus nsP2 independently governs viral RNA replication, cytopathicity, and inhibition of interferon signaling. Journal of virology 87:10394-10400.
14. Law Y-S, Utt A, Tan YB, Zheng J, Wang S, Chen MW, Griffin PR, Merits A, Luo D. 2019. Structural insights into RNA recognition by the Chikungunya virus nsP2 helicase. Proceedings of the National Academy of Sciences 116:9558-9567.
15. Das PK, Merits A, Lulla A. 2014. Functional cross-talk between distant domains of chikungunya virus non-structural protein 2 is decisive for its RNA-modulating activity. Journal of Biological Chemistry 289:5635-5653.
16. Ranji A, Boris-Lawrie K. 2010. RNA helicases: emerging roles in viral replication and the host innate response. RNA biology 7:775-787.
17. Law Y-S, Wang S, Tan YB, Shih O, Utt A, Goh WY, Lian B-J, Chen MW, Jeng U-S, Merits A. 2021. Interdomain flexibility of chikungunya virus nsP2 helicase-protease differentially influences viral RNA replication and infectivity. Journal of virology 95:10.1128/jvi. 01470-20.
18. Hall MC, Matson SW. 1999. Helicase motifs: the engine that powers DNA unwinding. Molecular microbiology 34:867-877.
19. Grimes SL, Denison MR. 2024. The Coronavirus helicase in replication. Virus Research 346:199401.
20. Singleton MR, Dillingham MS, Wigley DB. 2007. Structure and mechanism of helicases and nucleic acid translocases. Annu Rev Biochem 76:23-50.
21. Akhrymuk I, Kulemzin SV, Frolova EI. 2012. Evasion of the innate immune response: the Old World alphavirus nsP2 protein induces rapid degradation of Rpb1, a catalytic subunit of RNA polymerase II. Journal of virology 86:7180-7191.
22. Ranjith-Kumar C, Murali A, Dong W, Srisathiyanarayanan D, Vaughan R, Ortiz-Alacantara J, Bhardwaj K, Li X, Li P, Kao CC. 2009. Agonist and antagonist recognition by RIG-I, a cytoplasmic innate immunity receptor. Journal of Biological Chemistry 284:1155-1165.

23. Lu C, Xu H, Ranjith-Kumar C, Brooks MT, Hou TY, Hu F, Herr AB, Strong RK, Kao CC, Li P. 2010. The structural basis of 5′ triphosphate double-stranded RNA recognition by RIG-I C-terminal domain. Structure 18:1032-1043.
24. Ranjith-Kumar C, Lai Y, Sarisky RT, Cheng Kao C. 2010. Green tea catechin, epigallocatechin gallate, suppresses signaling by the dsRNA innate immune receptor RIG-I. PloS one 5:e12878.
25. Akhrymuk I, Frolov I, Frolova EI. 2018. Sindbis virus infection causes cell death by nsP2-induced transcriptional shutoff or by nsP3-dependent translational shutoff. Journal of virology 92:10.1128/jvi. 01388-18.
26. Meshram CD, Lukash T, Phillips AT, Akhrymuk I, Frolova EI, Frolov I. 2019. Lack of nsP2-specific nuclear functions attenuates chikungunya virus replication both in vitro and in vivo. Virology 534:14-24.
27. Madeira F, Madhusoodanan N, Lee J, Eusebi A, Niewielska A, Tivey AR, Lopez R, Butcher S. 2024. The EMBL-EBI Job Dispatcher sequence analysis tools framework in 2024. Nucleic acids research 52:W521-W525.
28. Akhrymuk I, Lukash T, Frolov I, Frolova EI. 2019. Novel mutations in nsP2 abolish chikungunya virus-induced transcriptional shutoff and make the virus less cytopathic without affecting its replication rates. Journal of virology 93:10.1128/jvi. 02062-18.
29. Abramson J, Adler J, Dunger J, Evans R, Green T, Pritzel A, Ronneberger O, Willmore L, Ballard AJ, Bambrick J. 2024. Accurate structure prediction of biomolecular interactions with AlphaFold 3. Nature 630:493-500.
30. Potter JA, Randall RE, Taylor GL. 2008. Crystal structure of human IPS-1/MAVS/VISA/Cardif caspase activation recruitment domain. BMC structural biology 8:1-10.
31. Kawai T, Takahashi K, Sato S, Coban C, Kumar H, Kato H, Ishii KJ, Takeuchi O, Akira S. 2005. IPS-1, an adaptor triggering RIG-I-and Mda5-mediated type I interferon induction. Nature immunology 6:981-988.
32. Hingane S, Joshi N, Surjit M, Ranjith-Kumar C. 2020. Hepatitis E virus ORF2 inhibits RIG-I mediated interferon response. Frontiers in microbiology 11:656.
33. Koyama S, Ishii KJ, Coban C, Akira S. 2008. Innate immune response to viral infection. Cytokine 43:336-341.
34. Lei J, Hilgenfeld R. 2017. RNA-virus proteases counteracting host innate immunity. FEBS letters 591:3190-3210.
35. Beachboard DC, Horner SM. 2016. Innate immune evasion strategies of DNA and RNA viruses. Current opinion in microbiology 32:113-119.
36. Bae S, Lee JY, Myoung J. 2019. Chikungunya virus-encoded nsP2, E2 and E1 strongly antagonize the interferon-β signaling pathway.
37. Kwong AD, Rao BG, Jeang K-T. 2005. Viral and cellular RNA helicases as antiviral targets. Nature reviews Drug discovery 4:845-853.
38. Frick D, Lam A. 2006. Understanding helicases as a means of virus control. Current pharmaceutical design 12:1315-1338.
39. Otsuka M, Kato N, Moriyama M, Taniguchi H, Wang Y, Dharel N, Kawabe T, Omata M. 2005. Interaction between the HCV NS3 protein and the host TBK1 protein leads to inhibition of cellular antiviral responses. Hepatology 41:1004-1012.
40. Riedl W, Acharya D, Lee J-H, Liu G, Serman T, Chiang C, Chan YK, Diamond MS, Gack MU. 2019. Zika virus NS3 mimics a cellular 14-3-3-binding motif to antagonize RIG-I-and MDA5-mediated innate immunity. Cell host & microbe 26:493-503. e6.
41. Gack MU, Diamond MS. 2016. Innate immune escape by Dengue and West Nile viruses. Current opinion in virology 20:119-128.

42. Feng K, Zhang HJ, Min YQ, Zhou M, Deng F, Wang HL, Li PQ, Ning YJ. 2023. SARS-CoV-2 NSP13 interacts with host IRF3, blocking antiviral immune responses. Journal of Medical Virology 95:e28881.
43. Fung S-Y, Siu K-L, Lin H, Chan C-P, Yeung ML, Jin D-Y. 2022. SARS-CoV-2 NSP13 helicase suppresses interferon signaling by perturbing JAK1 phosphorylation of STAT1. Cell & bioscience 12:36.
44. Setoh YX, Periasamy P, Peng NYG, Amarilla AA, Slonchak A, Khromykh AA. 2017. Helicase domain of West Nile virus NS3 protein plays a role in inhibition of type I interferon signalling. Viruses 9:326.
45. Fros JJ, Liu WJ, Prow NA, Geertsema C, Ligtenberg M, Vanlandingham DL, Schnettler E, Vlak JM, Suhrbier A, Khromykh AA. 2010. Chikungunya virus nonstructural protein 2 inhibits type I/II interferon-stimulated JAK-STAT signaling. Journal of virology 84:10877-10887.
46. Bouraï M, Lucas-Hourani M, Gad HH, Drosten C, Jacob Y, Tafforeau L, Cassonnet P, Jones LM, Judith D, Couderc T. 2012. Mapping of Chikungunya virus interactions with host proteins identified nsP2 as a highly connected viral component. Journal of virology 86:3121-3134.

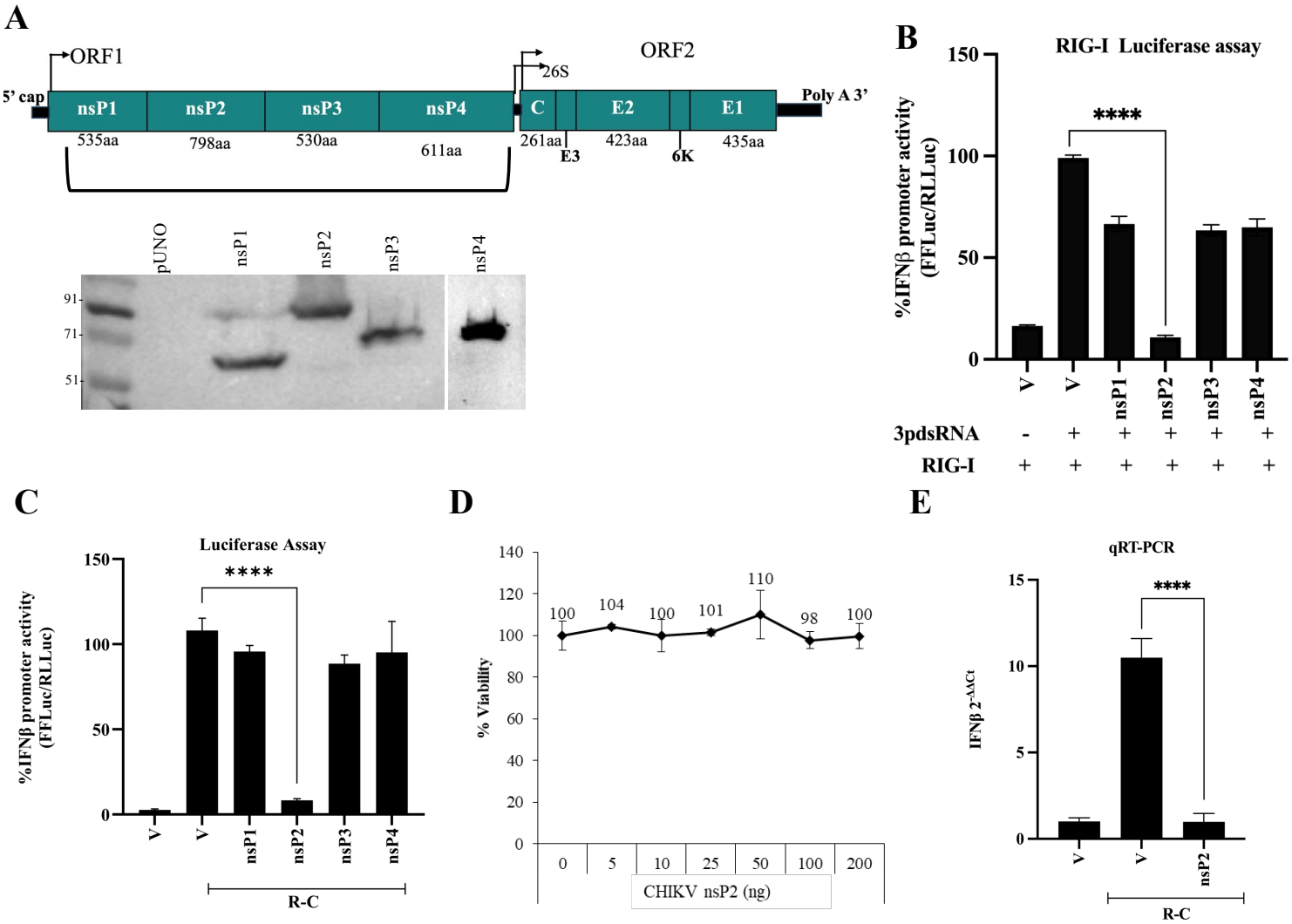

Figure 1:- CHIKV non-structural protein 2 (nsP2) inhibits RIG-I signaling. (A) Schematic representation of the CHIKV genome depicting nsPs and SPs. Western blot analysis of nsP1(~56kDa), nsP2(~89kDa), nsP3(~73kDa), nsP4(~72kDa) in HEK293T cells. (B) Dual luciferase assay to analyze RIG-I mediated IFN-β promoter activity, plasmids expressing nsP1(25ng), nsP2(25ng), nsP3(25ng), nsP4(25ng), and RIG-I (10ng) co-transfected along with IFN-β firefly and TK *Renilla* luciferase reporters in HEK293T cells, RIG-I was induced with 3p27dsRNA 24h post-transfection. Luciferase activity was measured post-16h induction. (C) Dual luciferase assay to analyze R-C mediated IFN-β promoter activity, plasmids (25ng) expressing nsP1, nsP2, nsP3, nsP4, and R-C (10ng) constitutively active CARD domain were co-transfected along with IFN-β firefly and TK *Renilla* luciferase reporters. (D) Cell viability assay-nsP2 plasmid at different amounts from 0 to 200 ng, transfected post 48h of transfection using WST-I reagent, absorbance measured at 450nm. Values were normalized to control absorbance measured at 630nm. (E) qRT-PCR to analyse IFNβ mRNA levels, HEK293T cells were co-transfected with R-C (100ng) and nsP2 (250ng) in a 12-well plate. Post 48h of transfection, RNA was isolated. Values are $2^{-\Delta\Delta Ct}$ ± SD for qRT PCR and mean percent ± SD for luciferase assay. n=3 for all experiments (**** denotes p value ≤ 0.001).

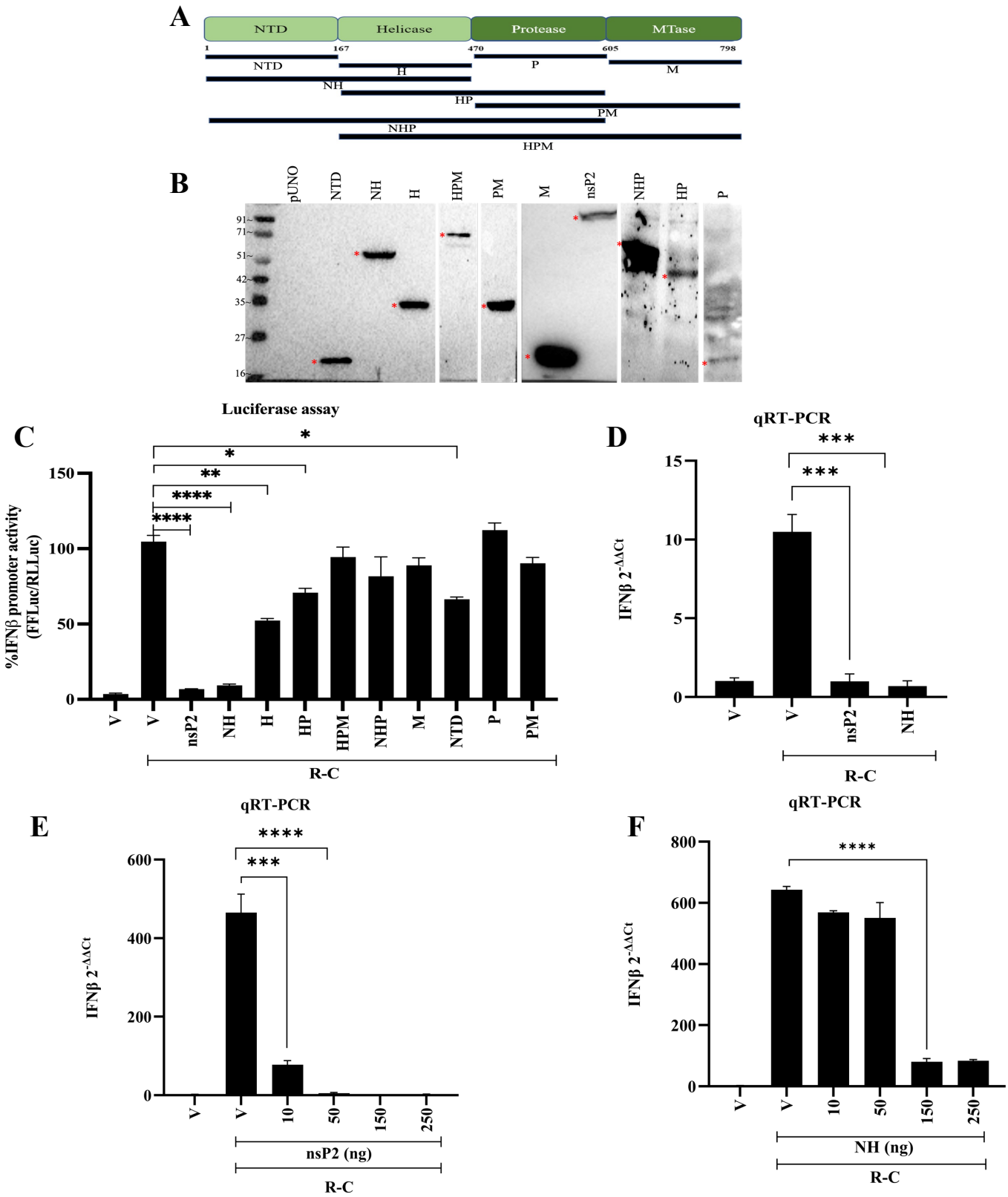

Figure 2: - NH (1-470 aa) of nsP2 inhibits RIG-I signaling (A) Schematic representation of CHIKV nsP2 subdomains, (B) Western Blot analysis of nsP2(89kDa), NTD(18kDa), H(34kDa), NH(56kDa), HP(48kDa), NHP(65kDa), HPM(70kDa), P(14kDa), PM(37kDa), M(22kDa) in HEK293T cells. (C) Dual luciferase assay to analyze R-C mediated IFN-β promoter activity, nsP2 (10ng), subdomains of nsP2(10ng), and R-C(10ng) along with IFN-β firefly and TK Renilla luciferase reporters co-transfected in HEK293T cells, and Luciferase activity was measured post 48h transfection. (D) qRT-PCR analysis of IFNβ mRNA levels in HEK293T cells co-transfected with R-C(100ng), nsP2(250ng), and NH(250ng). Post 48h of transfection, RNA was isolated. Ct values corresponding to IFNβ mRNA levels measured and normalized with GAPDH Ct values and change in mRNA levels was calculated by ΔΔCt method with respect to vector control. [E] For amount-dependent assay, HEK293T cells were transfected with increasing amounts of nsP2 and NH plasmid (10ng-250ng) in a 12-well plate. Post 48h of transfection, RNA was isolated. Values are $2^{-\Delta\Delta Ct}$ ± SD for qRT-PCR and mean percent ± SD for luciferase assay. n=3 for all experiments (**** denotes p value ≤ 0.001 * denotes p value ≤ 0.05).

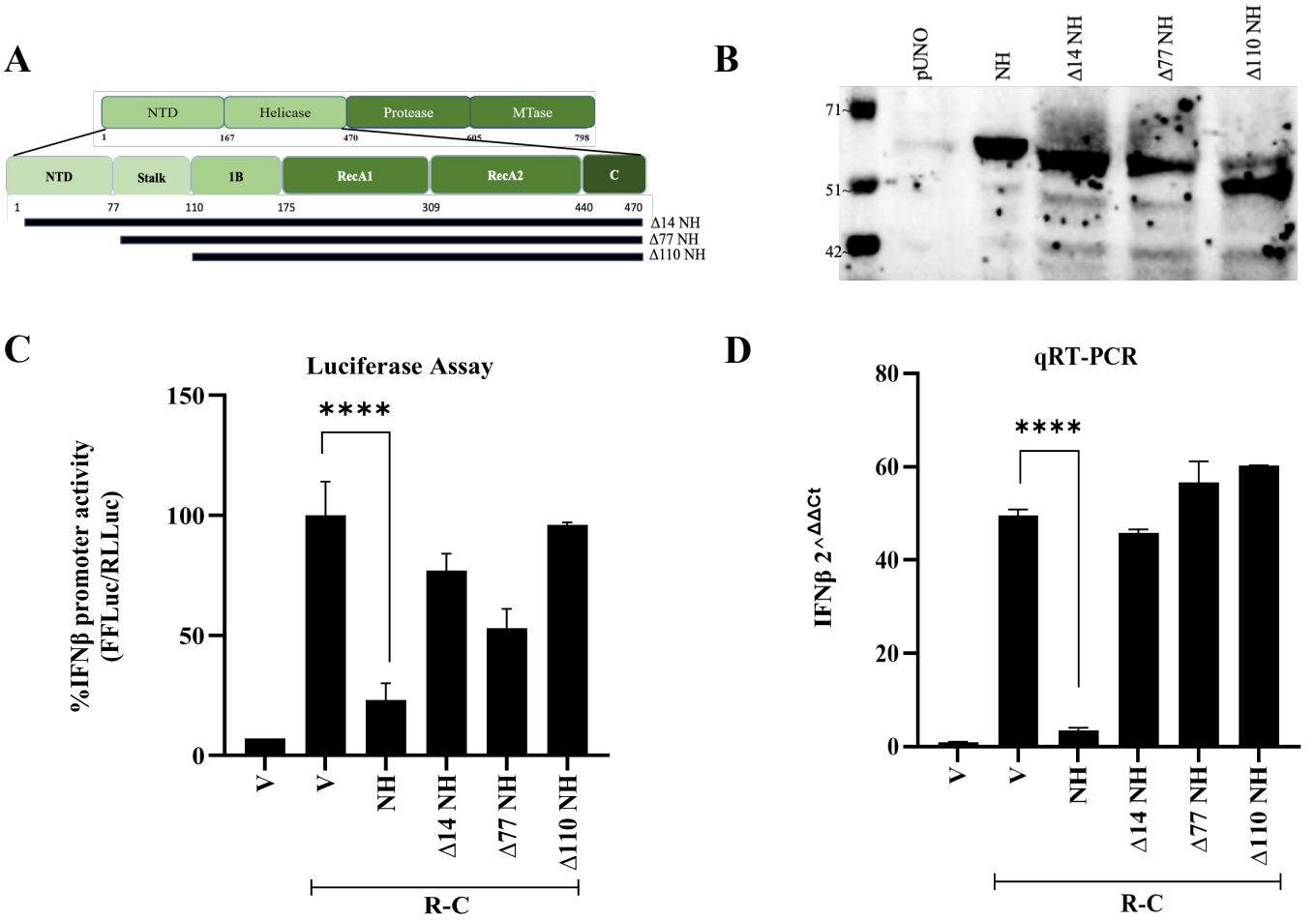

Figure 3:- nsP2-NH is the minimal region that inhibits RIG-I signaling (A) Schematic representation of CHIKV nsP2-NH subdomains, (B) Western Blot analysis of NH (~56kDa), Δ14 NH (~52kDa), Δ77 NH (~52kDa), and Δ110 NH (~49kDa) in HEK293T cells. (C) Dual luciferase assay to analyze R-C mediated IFN-β promoter activity, NH(25ng), Δ14 NH (25ng), Δ77 NH(25ng), and Δ110 NH(25ng), and R-C(10ng) along with IFN-β firefly and TK *Renilla* luciferase reporters co-transfected in HEK293T cells, and Luciferase activity was measured post 48h transfection. (D) qRT-PCR to analyse IFNβ mRNA levels, HEK293T cells co-transfected with R-C (100ng), NH (250ng), Δ14 NH (250ng), Δ77 NH (250ng), and Δ110 NH (250ng) in 12-well plate. Post 48h of transfection, RNA was isolated. Values are $2^{-\Delta\Delta Ct}$ ± SD for qRT PCR and mean percent ± SD for luciferase assay. n=3 for all experiments (**** denotes p value ≤ 0.001 * denotes p value ≤ 0.05).

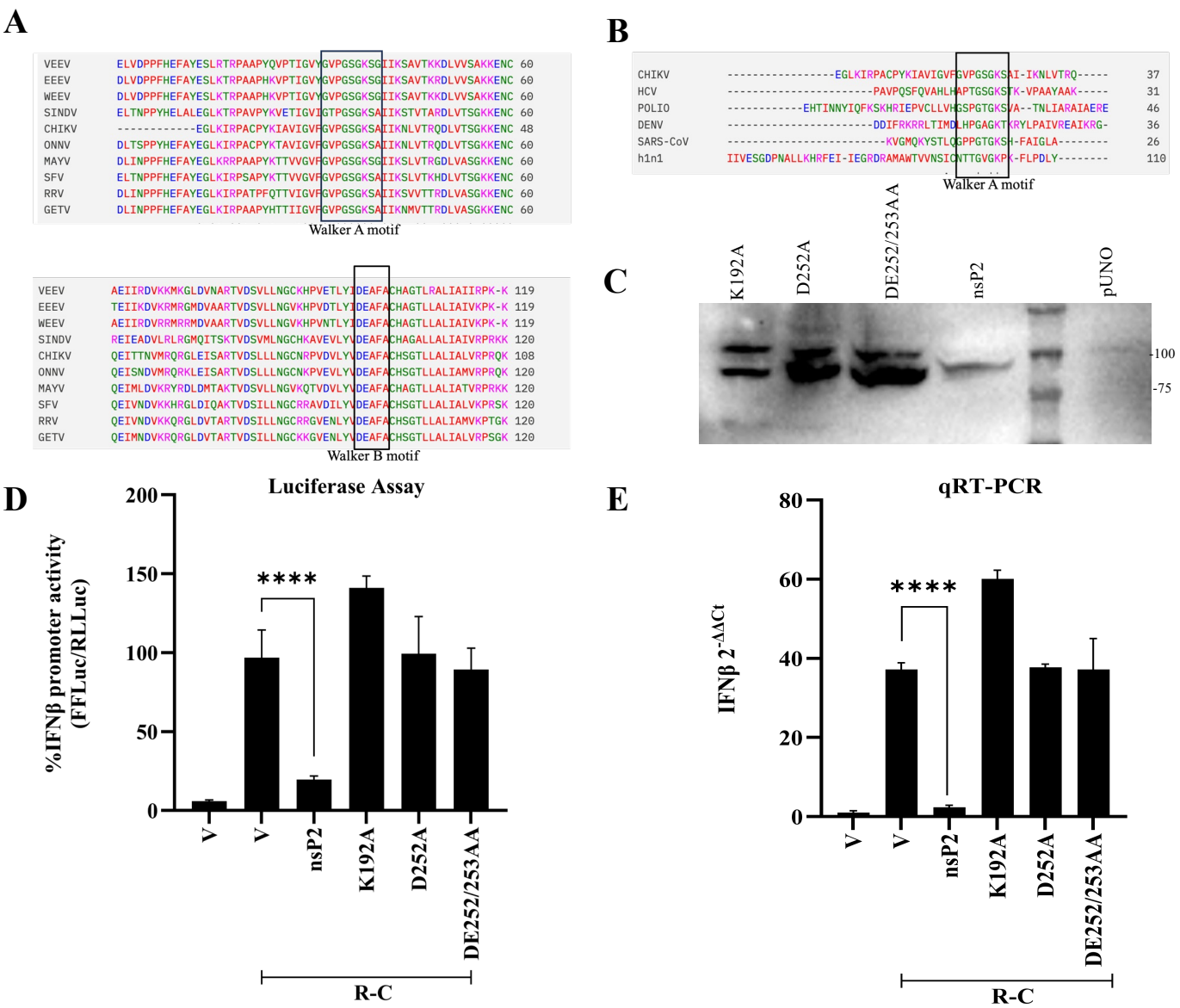

Figure 4:- nsP2 helicase mutant does not inhibit RIG-I signaling (A) Using Clustal Omega comparison of sequence encompassing aa residue (167aa- 470aa) of CHIKV nsP2 with other alphaviruses- Sindbis virus (SINV), O'nyong'nyong virus(ONNV), Eastern Equine Encephalitis virus (EEEV), Venezuelan equine encephalitis virus (VEEV), Western equine encephalitis virus (WEEV), and Mayaro virus (MAYV). The conserved walker motif regions are highlighted with a box. (B) The comparison of the nsP2 helicase domain with other viruses, PolioVirus, Hepatitis C Virus (HCV), Dengue virus (DENV), SARS-CoV-2, and H1N1 flu (swine flu), shows the conserved region of the Walker A motif. The highlighted helicase Walker motif A (186 aa-193 aa) and Walker motif B (252 aa -255 aa) are then mutated for analysis (C) Western Blot analysis of nsP2(~89kDa), K192A(~89kDa), D252A(~89kDa), and DE252/253AA(~89kDa) in HEK293T cells. (D) Dual luciferase assay to analyze R-C mediated IFN-β promoter activity, nsP2(25ng), K192A(25ng), D252A(25ng), and DE252/253AA(25ng), and R-C (10ng) along with IFN-β firefly and TK *Renilla* luciferase reporters co-transfected in HEK293T cells, and Luciferase activity was measured post 48h transfection. (D) qRT-PCR to analyse IFNβ mRNA levels, HEK293T cells co-transfected with R-C(100ng), nsP2 (250ng), K192A(250ng), D252A(250ng) and DE252/253AA(250ng) in 12-well plate. Post 48h of transfection, RNA was isolated. Values are $2^{-\Delta\Delta Ct}$ ± SD for qRT-PCR and mean percent ± SD for luciferase assay. n=3 for all experiments (**** denotes p value ≤ 0.001).

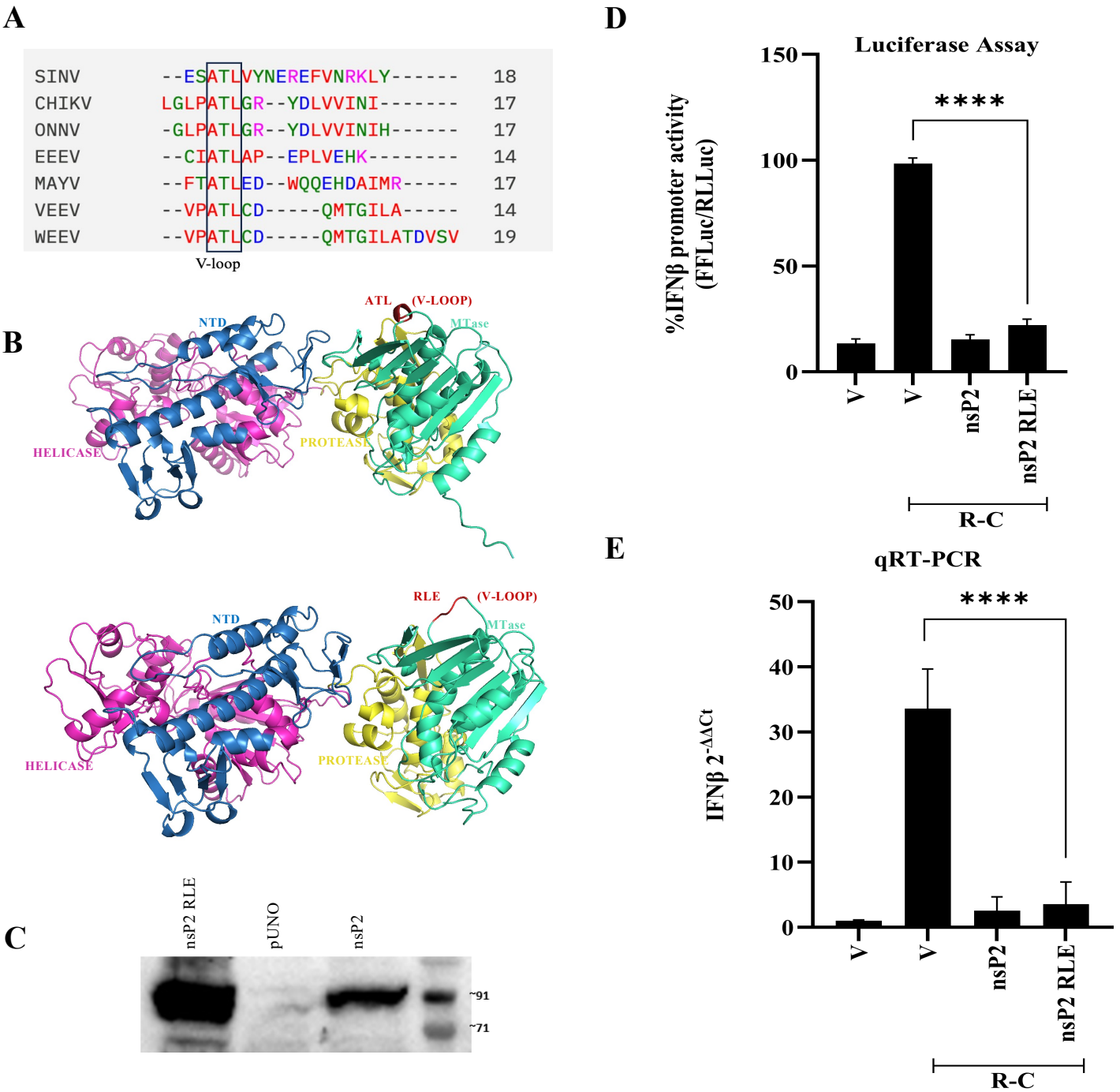

Figure 5:- nsP2 RLE mutant does inhibit RIG-I signaling (A) The sequence of CHIKV nsP2 C-terminal domain (605 aa- 798 aa) aligned with the C-terminal of Sindbis virus (SINV), O'nyong'nyong virus(ONNV), Eastern Equine Encephalitis virus (EEEV), Venezuelan equine encephalitis virus (VEEV), Western equine encephalitis virus (WEEV) , and Mayaro virus (MAYV). The highlighted conserved residues in all the sequences indicate a V-loop (ATL) region. (B) The predicted 3D structure of nsP2 using the Alphafold server shows the NTD (blue), Helicase (magenta), protease (yellow), and MTase domain (cyan). The ATL (V-Loop) of nsP2 is highlighted in red and mutated into RLE. (C) Western Blot analysis of nsP2 and RLE (~89kDa) in HEK293T cells. (D) Dual luciferase assay to analyze R-C mediated IFN-β promoter activity, nsP2(25ng), nsP2 RLE(25ng), and R-C (10ng) along with IFN-β firefly and TK *Renilla* luciferase reporters co-transfected in HEK293T cells, and Luciferase activity was measured post 48h transfection. (D) qRT-PCR to analyse IFNβ mRNA levels, HEK293T cells co-transfected with R-C(100ng), nsP2 (250ng), nsP2 RLE(250ng) in 12-well plate. Post 48h of transfection, RNA was isolated. Values are $2^{-\Delta\Delta Ct}$ ± SD for qRT-PCR and mean percent ± SD for luciferase assay. n=3 for all experiments (**** denotes p value ≤ 0.001).

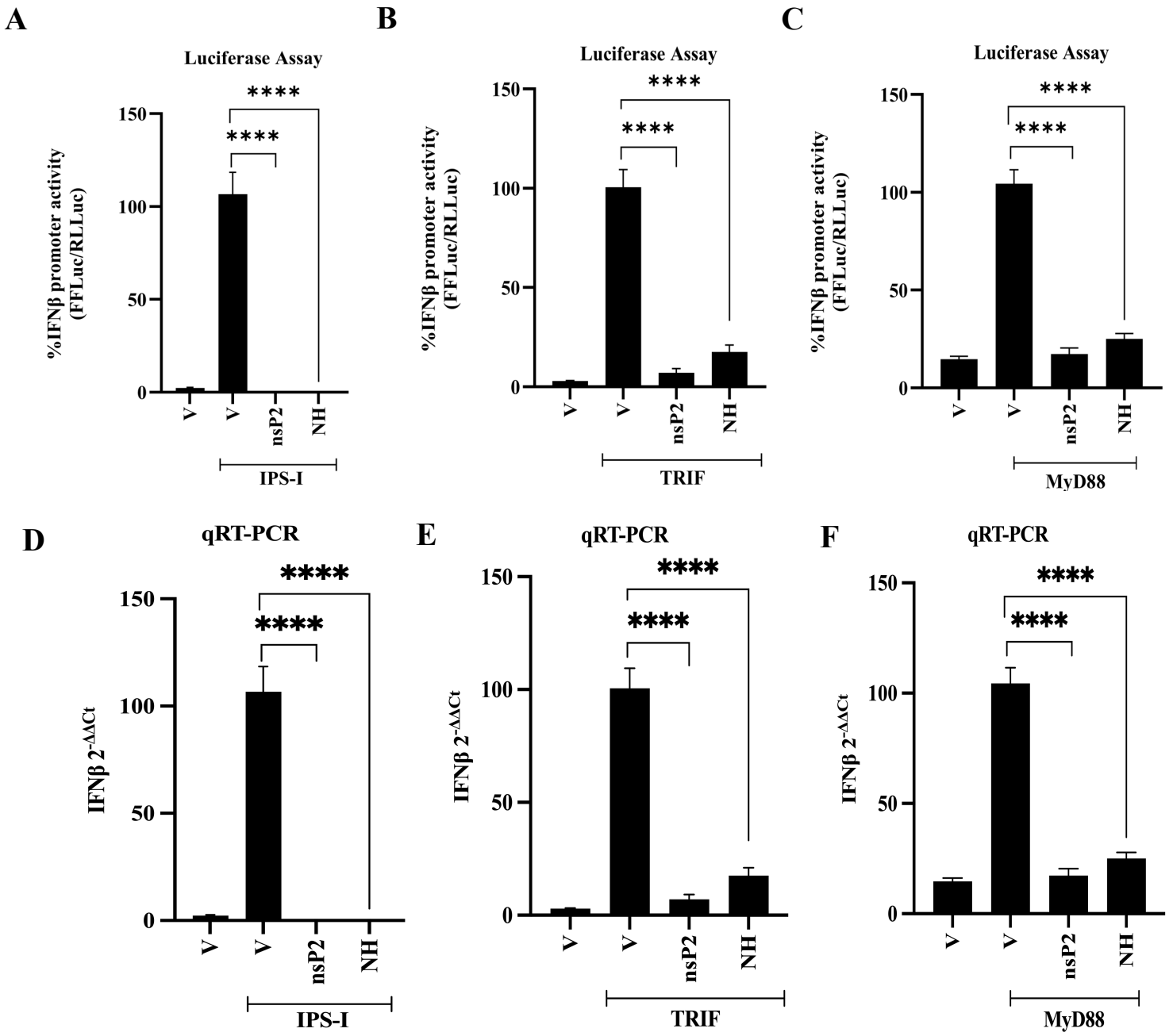

Figure 6:- nsP2 inhibits adaptor proteins of RIG-I and TLR signaling. Dual luciferase assay to analyze IPS-I (A), TRIF (B), and MyD88 (C) mediated IFN-β promoter activity, nsP2(25ng), NH(25ng), IPS-I(10ng), TRIF (25ng), MyD88 (25ng), along with IFN-β firefly and TK *Renilla* luciferase reporters co-transfected in HEK293T cells, and Luciferase activity was measured post 48h transfection. qRT-PCR to analyse IFNβ mRNA levels in IPS-I (D), TRIF (E), and MyD88 (F), HEK293T cells co-transfected with nsP2(250ng), NH(250ng), IPS-I(100ng), TRIF (250ng), MyD88 (250ng), in a 12-well plate. Post 48h of transfection, RNA was isolated. Values are mean percent ± SD for the luciferase assay. n=3 for all experiments (**** denotes p value ≤ 0.001). Values are $2^{-\Delta\Delta Ct}$ ± SD for qRT PCR and mean percent ± SD for luciferase assay. n=3 for all experiments (**** denotes p value ≤ 0.001)

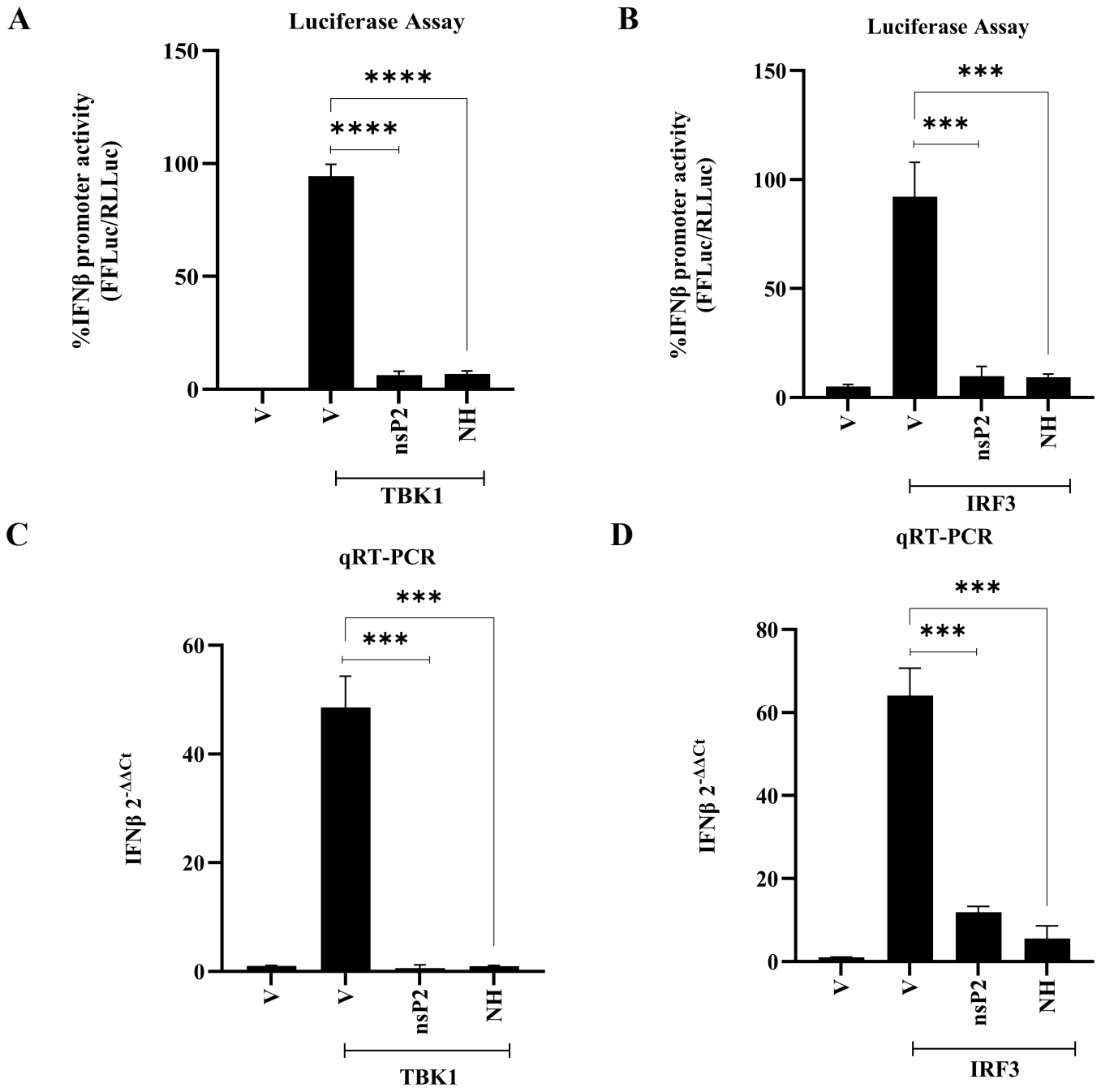

Figure 7:- nsP2 and NH inhibit TBK1 and IRF3-induced signaling. (A), (B) Dual luciferase assay to analyze TBK1, IRF3-mediated IFN-β promoter activity, nsP2(25ng), NH(25ng), TBK1(25ng), IRF3(25ng), along with IFN-β firefly and TK *Renilla* luciferase reporters co-transfected. (C), (D) qRT-PCR to analyse IFNβ mRNA levels, HEK293T cells co-transfected with TBK1(250ng), IRF3(250ng), nsP2 (250ng), NH(250ng) in 12-well plate. Post 48h of transfection, RNA was isolated. Values are $2^{-\Delta\Delta Ct}$ ± SD for qRT-PCR and mean percent ± SD for luciferase assay. n=3 for all experiments (**** denotes p value ≤ 0.001).